40. PLOTS OF CROSS SECTIONS AND RELATED QUANTITIES

Jet Production in pp and $\overline{p}p$ Interactions

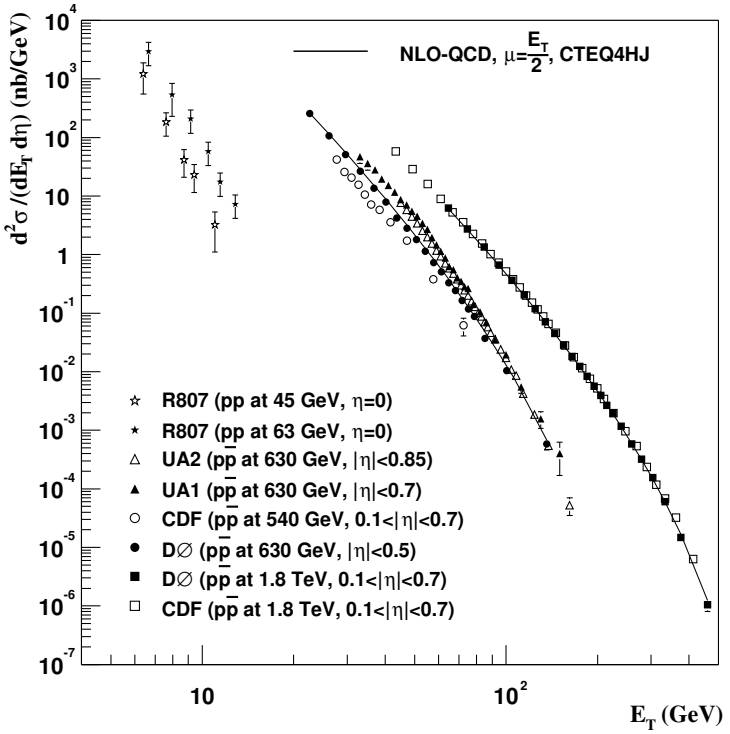

Figure 40.1: Transverse energy dependence of the inclusive differential jet cross sections in the central pseudorapidity region. The error bars are either statistical (DØ), statistical and p_T dependent (UA2), statistical and energy dependent from unsmearing (UA1), uncorrelated (CDF), or total (R806) uncertainties. Comparison of the different experimental results is not straight forward, since the different experiments used different jet reconstruction algorithms. For instance, DØ and CDF used a fixed cone algorithm with a size $\mathcal{R}$=0.7 for all their measurements, compared to a cone size of 1.3 for UA2. **DØ**: Phys. Rev. **D64**, 032003 (2001); **CDF**: Phys. Rev. **D64**, 032001 (2001); **UA1**: Phys. Lett. **B172**, 461 (1986); **UA2**: Phys. Lett. **B257**, 232 (1991); **R807**: Phys. Lett. **B123**, 133 (1983). Next-to-Leading order QCD predictions, using CTEQ4HJ pdfs and $\mu_{R,F} = E_T/2$, are shown for $p\overline{p}$ at 630 GeV and 1.8 TeV. (Courtesy of V.D. Elvira, Fermilab, 2001)

Direct γ Production in $\overline{p}p$ Interactions

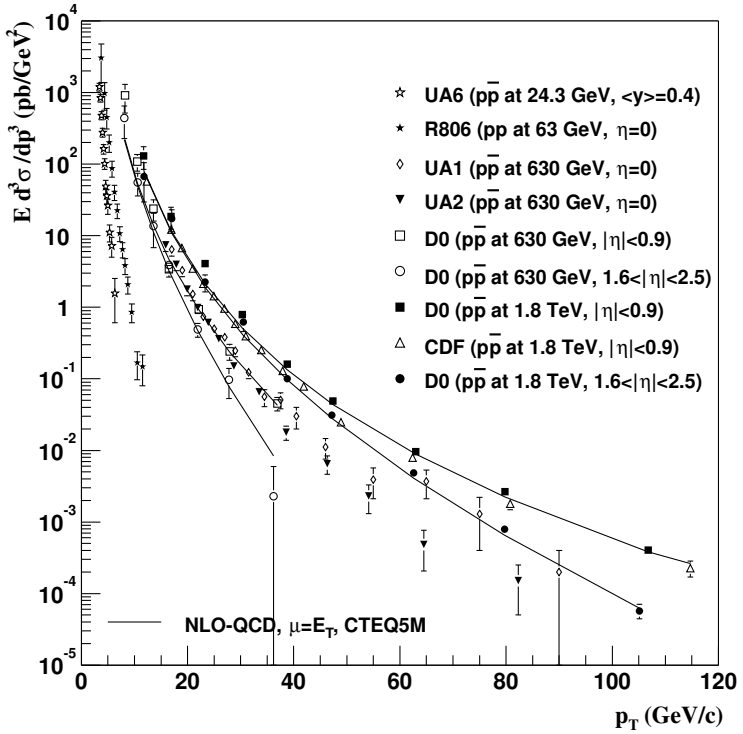

Figure 40.2: Transverse energy dependence of isolated photon cross sections. The error bars are either statistical (CDF), uncorrelated (DØ), or total (UA1, UA2, R806) uncertainties. **DØ**: Phys. Rev. Lett. **87**, 251805 (2001); **CDF**: Phys. Rev. **D73**, 2662 (1994); **UA6**: Phys. Lett. **B206**, 163 (1988); **UA1**: Phys. Lett. **B209**, 385 (1988); **UA2**: Phys. Lett. **B288**, 386 (1992); **R806**: Z. Phys. **C13**, 277 (1982). Next-to-Leading order QCD predictions are shown for $p\overline{p}$ at 630 GeV and 1.8 TeV. (Courtesy of V.D. Elvira, Fermilab, 2001)

Differential Cross Section for W and Z Boson Production

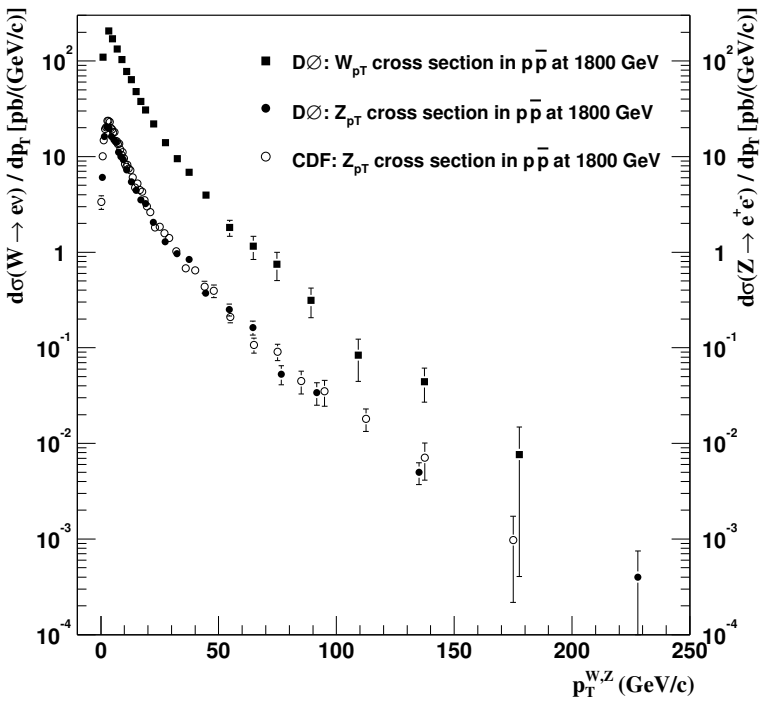

Figure 40.3: Differential cross section for W and Z boson production. The error bars are total errors, excluding the DØ (CDF) 4.4% (3.9%) luminosity uncertainty. **DØ**: Phys. Lett. **B513**, 292 (2001), Phys. Rev. Lett. **84**, 2792 (2000). **CDF**: Phys. Rev. Lett. **84**, 845 (2000). (Courtesy of V.D. Elvira, Fermilab, 2001)

Pseudorapidity Distributions in $\overline{p}p$ Interactions

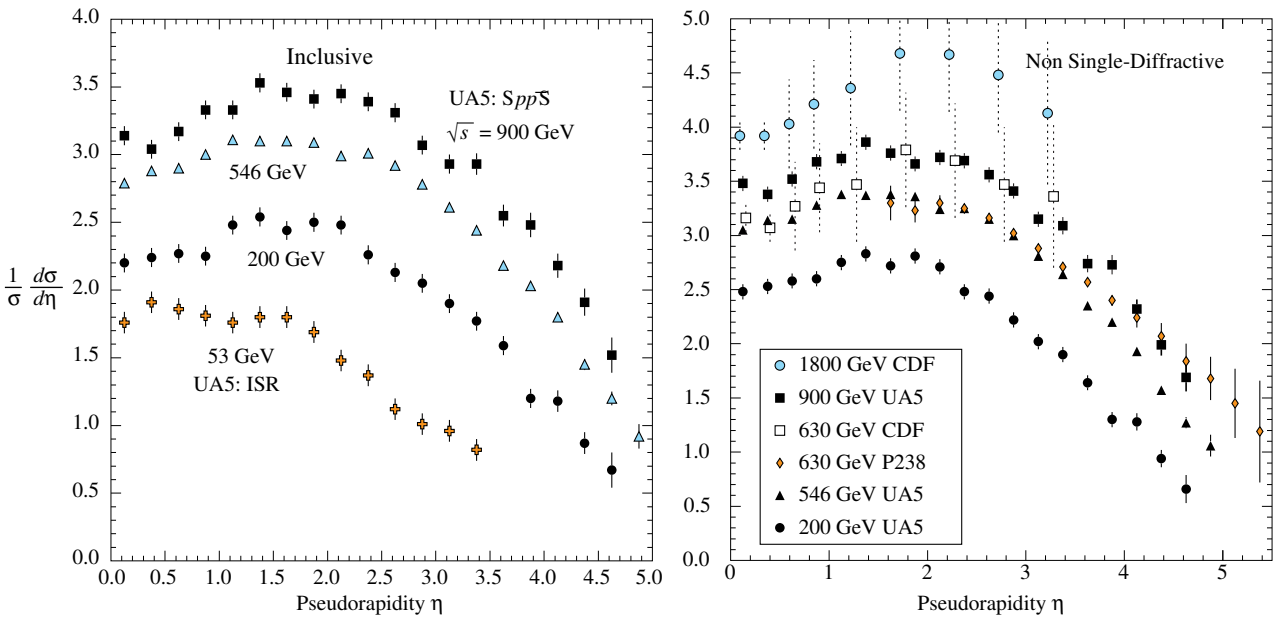

Figure 40.4: Charged particle pseudorapidity distributions in $p\overline{p}$ collisions for 53 GeV $\leq \sqrt{s} \leq$ 1800 GeV. UA5 data from the S$p\overline{p}$S are taken from G.J. Alner *et al.*, Z. Phys. **C33**, 1 (1986), and from the ISR from K. Alpgøard *et al.*, Phys. Lett. **112B**, 193 (1982). The UA5 data are shown for both the full inelastic cross-section and with singly diffractive events excluded. Additional non single-diffractive measurements are available from CDF at the Tevatron, F. Abe *et al.*, Phys. Rev. **D41**, 2330 (1990) and Experiment P238 at the S$\overline{p}p$S, R. Harr *et al.*, Phys. Lett. **B401**, 176 (1997). (Courtesy of D.R. Ward, Cambridge Univ., 1999.)

Average Hadron Multiplicities in Hadronic e^+e^- Annihilation Events

Table 40.1: Average hadron multiplicities per hadronic e^+e^- annihilation event at $\sqrt{s} \approx 10$, 29–35, 91, and 130–200 GeV. The rates given include decay products from resonances with $c\tau < 10$ cm, and include the corresponding anti-particle state. Correlations of the systemaic uncertainties were considered for the calculation of the averages. (Updated July 2003 by O. Biebel, LMU, Munich.)

Particle	$\sqrt{s} \approx 10$ GeV	$\sqrt{s} = 29$–35 GeV	$\sqrt{s} = 91$ GeV	$\sqrt{s} = 130$–200 GeV
Pseudoscalar mesons:				
π^+	6.6 ± 0.2	10.3 ± 0.4	16.99 ± 0.27	21.24 ± 0.39
π^0	3.2 ± 0.3	5.83 ± 0.28	9.42 ± 0.32	
K^+	0.90 ± 0.04	1.48 ± 0.09	2.242 ± 0.063	2.81 ± 0.19
K^0	0.91 ± 0.05	1.48 ± 0.07	2.049 ± 0.026	2.10 ± 0.12
η	0.20 ± 0.04	0.61 ± 0.07	1.049 ± 0.080	
$\eta'(958)$	0.03 ± 0.01	0.26 ± 0.10	0.152 ± 0.020	
D^+	$0.16 \pm 0.03^{(k)}$	0.17 ± 0.03	0.175 ± 0.016	
D^0	$0.37 \pm 0.06^{(k)}$	0.45 ± 0.07	0.454 ± 0.030	
D_s^+	$0.13 \pm 0.02^{(k)}$	$0.45 \pm 0.20^{(a)}$	0.131 ± 0.021	
B^+, B_d^0	—	—	$0.165 \pm 0.026^{(b)}$	
B_s^0	—	—	$0.057 \pm 0.013^{(b)}$	
Scalar mesons:				
$f_0(980)$	0.024 ± 0.006	$0.05 \pm 0.02^{(c)}$	0.146 ± 0.012	
$a_0(980)^\pm$	—	—	$0.27 \pm 0.11^{(d)}$	
Vector mesons:				
$\rho(770)^0$	0.35 ± 0.04	0.81 ± 0.08	1.231 ± 0.098	
$\rho(770)^\pm$	—	—	$2.40 \pm 0.43^{(d)}$	
$\omega(782)$	0.30 ± 0.08	—	1.016 ± 0.065	
$K^*(892)^+$	0.27 ± 0.03	0.64 ± 0.05	0.715 ± 0.059	
$K^*(892)^0$	0.29 ± 0.03	0.56 ± 0.06	0.738 ± 0.024	
$\phi(1020)$	0.044 ± 0.003	0.085 ± 0.011	0.0963 ± 0.0032	
$D^*(2010)^+$	$0.22 \pm 0.04^{(k)}$	0.43 ± 0.07	$0.1937 \pm 0.0057^{(j)}$	
$D^*(2007)^0$	$0.23 \pm 0.06^{(k)}$	0.27 ± 0.11	—	
$D_s^*(2112)^+$	—	—	$0.101 \pm 0.048^{(f)}$	
$B^{*\ (g)}$	—	—	0.288 ± 0.026	
$J/\psi(1S)$	$0.00050 \pm 0.00005^{(k)}$	—	$0.0052 \pm 0.0004^{(h)}$	
$\psi(2S)$	—	—	$0.0023 \pm 0.0004^{(h)}$	
$\Upsilon(1S)$	—	—	$0.00014 \pm 0.00007^{(h)}$	
Pseudovector mesons:				
$\chi_{c1}(3510)$	—	—	$0.0041 \pm 0.0011^{(h)}$	
Tensor mesons:				
$f_2(1270)$	0.09 ± 0.02	0.14 ± 0.04	0.166 ± 0.020	
$f_2'(1525)$	—	—	0.012 ± 0.006	
$K_2^*(1430)^+$	—	0.09 ± 0.03	—	
$K_2^*(1430)^0$	—	0.12 ± 0.06	$0.084 \pm 0.022^{(h)}$	
$B^{**\ (i)}$	—	—	0.118 ± 0.024	
$D_{s1}^\pm$	—	—	$0.0052 \pm 0.0011^{(\ell)}$	
$D_{s2}^{*\pm}$	—	—	$0.0083 \pm 0.0031^{(\ell)}$	
Baryons:				
p	0.253 ± 0.016	0.640 ± 0.050	1.048 ± 0.045	1.41 ± 0.18
Λ	0.080 ± 0.007	0.205 ± 0.010	0.3915 ± 0.0065	0.39 ± 0.03
Σ^0	0.023 ± 0.008	—	0.076 ± 0.011	
Σ^-	—	—	0.081 ± 0.010	
Σ^+	—	—	0.107 ± 0.011	
$\Sigma^\pm$	—	—	0.174 ± 0.009	
Ξ^-	0.0059 ± 0.0007	0.0176 ± 0.0027	0.0258 ± 0.0010	
$\Delta(1232)^{++}$	0.040 ± 0.010	—	0.085 ± 0.014	
$\Sigma(1385)^-$	0.006 ± 0.002	0.017 ± 0.004	0.0240 ± 0.0017	
$\Sigma(1385)^+$	0.005 ± 0.001	0.017 ± 0.004	0.0239 ± 0.0015	
$\Sigma(1385)^\pm$	0.0106 ± 0.0020	0.033 ± 0.008	0.0462 ± 0.0028	
$\Xi(1530)^0$	0.0015 ± 0.0006	—	0.0055 ± 0.0005	
Ω^-	0.0007 ± 0.0004	0.014 ± 0.007	0.0016 ± 0.0003	
Λ_c^+	$0.100 \pm 0.030^{(j)}$	0.110 ± 0.050	0.078 ± 0.017	
Λ_b^0	—	—	0.031 ± 0.016	
$\Sigma_c^{++}, \Sigma_c^0$	0.014 ± 0.007	—	—	
$\Lambda(1520)$	0.008 ± 0.002	—	0.0222 ± 0.0027	

Notes for Table 40.1:

(*a*) B($D_s \to \eta\pi,\ \eta'\pi$) was used (RPP1994).

(*b*) The Standard Model B($Z \to b\bar{b}$) = 0.217 was used.

(*c*) $x_p = p/p_{\rm beam} > 0.1$ only.

(*d*) Both charge states.

(*e*) B($D^*(2010)^+ \to D^0\pi^+$) × B($D^0 \to K^-\pi^+$) has been used (RPP2000).

(*f*) B($D_s^* \to D_S^+\gamma$), B($D_s^+ \to \phi\pi^+$), B($\phi \to K^+K^-$) have been used (RPP1998).

(*g*) Any charge state (*i.e.*, B_d^*, B_u^*, or B_s^*).

(*h*) B($Z \to$ hadrons) = 0.699 was used (RPP1994).

(*i*) Any charge state (*i.e.*, B_d^{**}, B_u^{**}, or B_s^{**}).

(*j*) The value was derived from the cross section of $\Lambda_c^+ \to p\pi K$, assuming the branching fraction to be $(3.2 \pm 0.7)\%$ (RPP1992).

(*k*) $\sigma_{\rm had} = 3.33 \pm 0.05 \pm 0.21$ nb (**CLEO**: Phys. Rev. **D29**, 1254 (1984)) has been used in converting the measured cross sections to average hadron multiplicities.

(*ℓ*) Assumes B($D_{s1}^+ \to D^{*+}K^0 + D^{*0}K+$) = 100% and B($D_{s2}^+ \to D^0K^+$) = 45%.

References for Table 40.1:

RPP1992: Phys. Rev. **D45** (1992) and references therein.

RPP1994: Phys. Rev. **D50**, 1173 (1994) and references therein.

RPP1996: Phys. Rev. **D54**, 1 (1996) and references therein.

RPP1998: Eur. Phys. J. **C3**, 1 (1998) and references therein.

RPP2000: Eur. Phys. J. **C15**, 1 (2000) and references therein.

RPP2002: Phys. Rev. **D66**, 010001 (2002) and references therein.

R. Marshall, Rep. Prog. Phys. **52**, 1329 (1989)

A. De Angelis, J. Phys. **G19**, 1233 (1993) and references therein.

ALEPH: D. Buskulic *et al.*: Phys. Lett. **B295**, 396 (1992); Z. Phys. **C64**, 361 (1994); **C69**, 15 (1996); **C69**, 379 (1996); **C73**, 409 (1997); and
R. Barate *et al.*: Z. Phys. **C74**, 451 (1997); Phys. Reports **294**, 1 (1998); Eur. Phys. J. **C5**, 205 (1998); **C16**, 597 (2000); **C16**, 613 (2000); and
A. Heister *et al.*: Phys. Lett. **B526**, 34 (2002); **B528**, 19 (2002).

ARGUS: H. Albrecht *et al.*: Phys. Lett. **230B**, 169 (1989); Z. Phys. **C44**, 547 (1989); **C46**, 15 (1990); **C54**, 1 (1992); **C58**, 199 (1993); **C61**, 1 (1994); Phys. Rep. **276**, 223 (1996).

BaBar: B. Aubert *et al.*: Phys. Rev. Lett. **87**, 162002 (2001).

Belle: K. Abe *et al.*: Phys. Rev. Lett. **88**, 052001 (2002).

CELLO: H.J. Behrend *et al.*: Z. Phys. **C46**, 397 (1990); **C47**, 1 (1990).

CLEO: D. Bortoletto *et al.*, Phys. Rev. **D37**, 1719 (1988).

Crystal Ball: Ch. Bieler *et al.*, Z. Phys. **C49**, 225 (1991).

DELPHI: P. Abreu *et al.*: Z. Phys. **C57**, 181 (1993); **C59**, 533 (1993); **C61**, 40 7(1994); **C65**, 587 (1995); **C67**, 543 (1995); **C68**, 353 (1995); **C73**, 61 (1996); Nucl. Phys. **B444**, 3 (1995); Phys. Lett. **B341**, 109 (1994); **B345**, 598 (1995); **B361**, 207 (1995); **B372**, 172 (1996); **B379**, 309 (1996); **B416**, 233 (1998); **B449**, 364 (1999); **B475**, 429 (2000); Eur. Phys. J. **C6**, 19 (1999); **C5**, 585 (1998); **C18**, 203 (2000).

HRS: S. Abachi *et al.*, Phys. Rev. Lett. **57**, 1990 (1986); and
M. Derrick *et al.*, Phys. Rev. **D35**, 2639 (1987).

L3: M. Acciarri *et al.*: Phys. Lett. **B328**, 223 (1994); **B345**, 589 (1995); **B371**, 126 (1996); **B371**, 137 (1996); **B393**, 465 (1997); **B404**, 390 (1997); **B407**, 351 (1997); **B407**, 389 (1997), erratum ibid. **B427**, 409 (1998); **B453**, 94 (1999); **B479**, 79 (2000).

MARK II: H. Schellman *et al.*, Phys. Rev. **D31**, 3013 (1985); and
G. Wormser *et al.*, Phys. Rev. Lett. **61**, 1057 (1988).

JADE: W. Bartel *et al.*, Z. Phys. **C20**, 187 (1983); andD.D. Pietzl *et al.*, Z. Phys. **C46**, 1 (1990).

OPAL: R. Akers *et al.*: Z. Phys. **C63**, 181 (1994); **C66**, 555 (1995); **C67**, 389 (1995); **C68**, 1 (1995); and
G. Alexander *et al.*: Phys. Lett. **B358**, 162 (1995); Z. Phys. **C70**, 197 (1996); **C72**, 1 (1996); **C72**, 191 (1996); **C73**, 569 (1997); **C73**, 587 (1997); Phys. Lett. **B370**, 185 (1996); and
K. Ackerstaff *et al.*: Z. Phys. **C75**, 192 (1997); Phys. Lett. **B412**, 210 (1997); Eur. Phys. J. **C1**, 439 (1998); **C4**, 19 (1998); **C5**, 1 (1998); **C5**, 411 (1998); and
G. Abbiendi *et al.*: Eur. Phys. J. **C16**, 185 (2000); **C16**, 185 (2000).

PLUTO: Ch. Berger *et al.*, Phys. Lett. **104B**, 79 (1981).

SLD: K. Abe, Phys. Rev. **D59**, 052001 (1999).

TASSO: H. Aihara *et al.*, Z. Phys. **C27**, 27 (1985).

TPC: H. Aihara *et al.*, Phys. Rev. Lett. **53**, 2378 (1984).

Average e^+e^-, pp, and $\overline{p}p$ Multiplicity

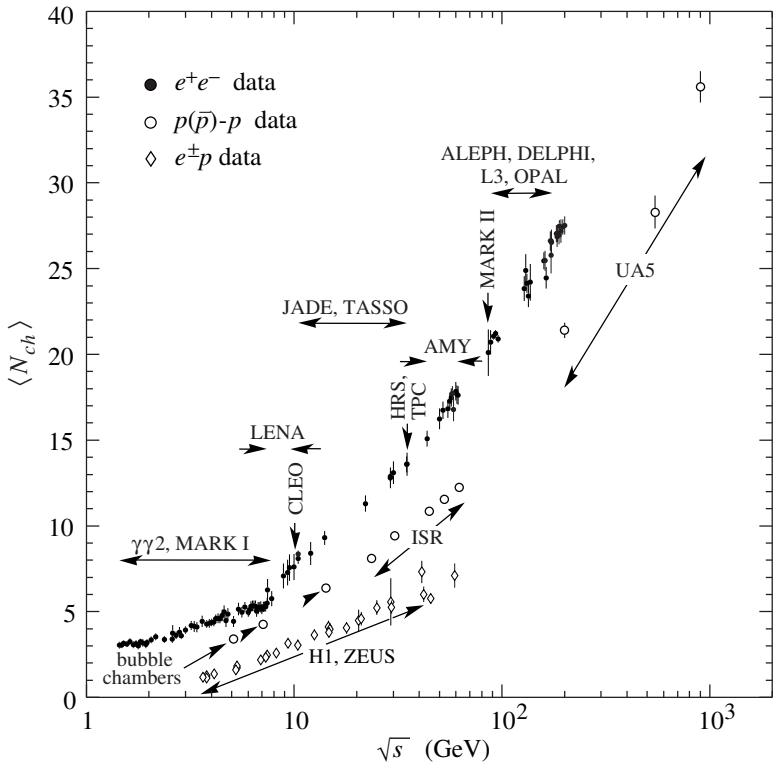

Figure 40.5: Average multiplicity as a function of $\sqrt{s}$ for e^+e^- and $p\overline{p}$ annihilations, and pp and ep collisions. The indicated errors are statistical and systematic errors added in quadrature, except when no systematic errors are given. Files of the data shown in this figure are given in `http://home.cern.ch/b/biebel/www/RPP02`

—

e^+e^-: Most e^+e^- measurements include contributions from K^0_S and Λ decays. The $\gamma\gamma 2$ and MARK I measurements contain a systematic 5% error. Points at identical energies have been spread horizontally for clarity:

ALEPH: D. Buskulic *et al.*, Z. Phys. **C69**, 15 (1995); and Z. Phys. **C73**, 409 (1997).

ARGUS: H. Albrecht *et al.*, Z. Phys. **C54**, 13 (1992).

DELPHI: P. Abreu *et al.*, Eur. Phys. J. **C6**, 19 (1999); Phys. Lett. **B372**, 172 (1996); Phys. Lett. **B416**, 233 (1998); and Eur. Phys. J. **C18**, 203 (2000).

L3: M. Acciarri *et al.*, Phys. Lett. **B371**, 137 (1996); Phys. Lett. **B404**, 390 (1997); and Phys. Lett. **B444**, 569 (1998).

OPAL: G. Abbiendi *et al.*, Eur. Phys. J. **C16**, 185 (2000);
K. Ackerstaff *et al.*, Z. Phys. **C75**, 193 (1997);
P.D. Acton *et al.*, Z. Phys. **C53**, 539 (1992) and references therein;
R. Akers *et al.*, Z. Phys. **C68**, 203 (1995).

TOPAZ: K. Nakabayashi *et al.*, Phys. Lett. **B413**, 447 (1997).

VENUS: K. Okabe *et al.*, Phys. Lett. **B423**, 407 (1998).

—

$e^{\pm}p$: Multiplicities have been measured in the current fragmentation region of the Breit frame:

H1: C. Adloff *et al.*, Nucl. Phys. **B504**, 3 (1997).

ZEUS: J. Breitweg *et al.*, Eur. Phys. J. **C11**, 251 (1999);
S. Chekanov *et al.*, Phys. Lett. **B510**, 36 (2001).

—

$p(\overline{p})$: The errors of the $p(\overline{p})$ measurements are the quadratically added statistical and systematic errors, except for the bubble chamber measurements for which only statistical errors are given in the references. The values measured by UA5 exclude single diffractive dissociation:

—

bubble chamber: J. Benecke *et al.*, Nucl. Phys. **B76**, 29 (1976); W.M. Morse *et al.*, Phys. Rev. **D15**, 66 (1977).

ISR: A. Breakstone *et al.*, Phys. Rev. **D30**, 528 (1984).

UA5: G.J. Alner *et al.*, Phys. Lett. **167B**, 476 (1986);
R.E. Ansorge *et al.*, Z. Phys. **C43**, 357 (1989).

(Courtesy of O. Biebel, MPI München, 2001.)

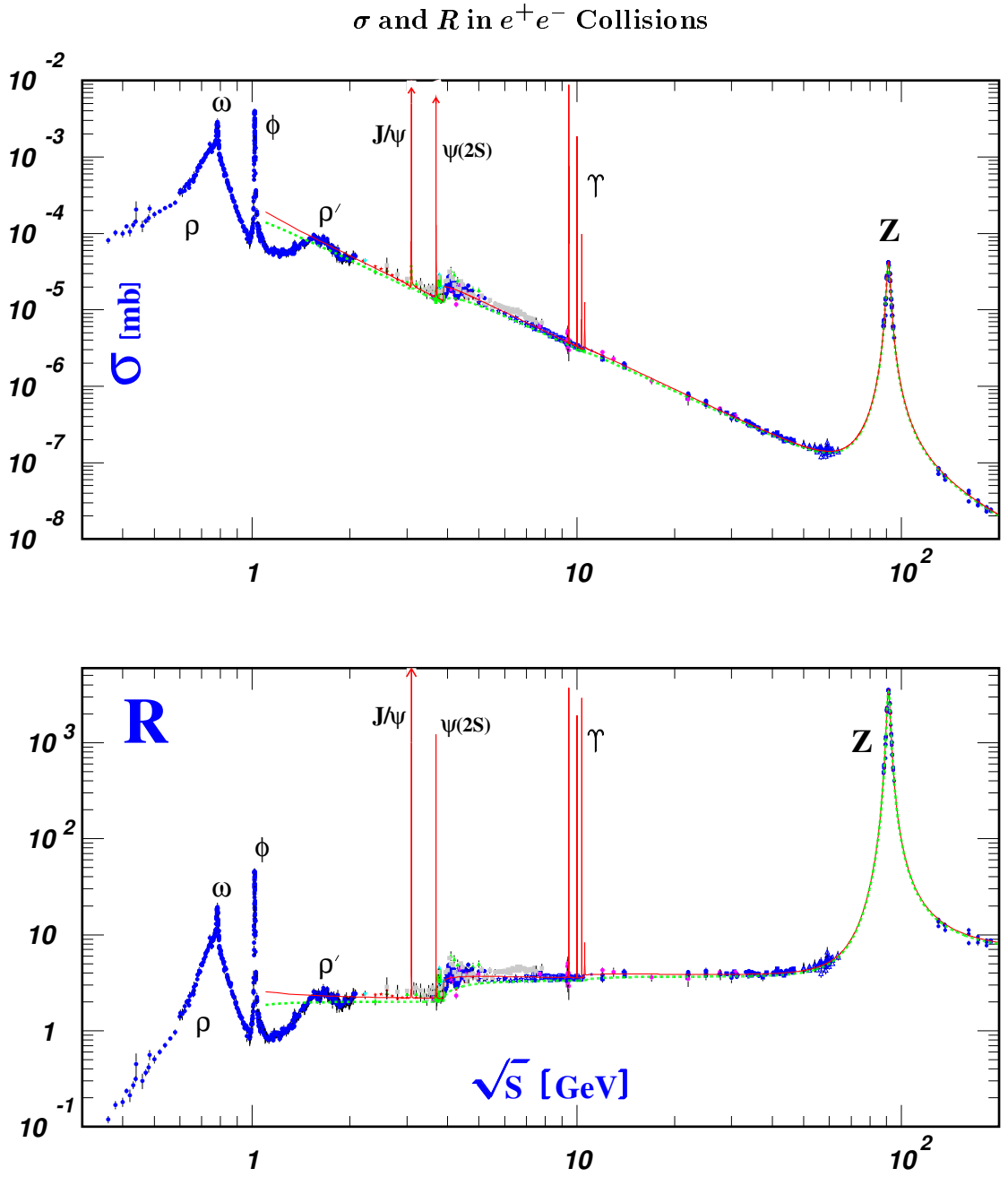

Figure 40.6: World data on the total cross section of $e^+e^- \to hadrons$ and the ratio $R(s) = \sigma(e^+e^- \to hadrons, s)/\sigma(e^+e^- \to \mu^+\mu^-, s)$. $\sigma(e^+e^- \to hadrons, s)$ is the experimental cross section corrected for initial state radiation and electron-positron vertex loops, $\sigma(e^+e^- \to \mu^+\mu^-, s) = 4\pi\alpha^2(s)/3s$. Data errors are total below 2 GeV and statistical above 2 GeV. The curves are an educative guide: the broken one is a naive quark-parton model prediction and the solid one is 3-loop pQCD prediction (see "Quantum Chromodynamics" section of this *Review*, Eq. (9.12) or, for more details, K. G. Chetyrkin et al., `hep-ph/0005139`, p.3, Eqs. (1)-(3)). Breit-Wigner parameterizations of J/ψ, $\psi(2S)$, and $\Upsilon(nS), n = 1..4$ are also shown. **Note:** The experimental shapes of these resonances are dominated by machine energy spread and are not shown. The full list of references to the original data and the details of the R ratio extraction from them can be found in `hep-ph/0312114`. Corresponding computer-readable data files are available at `http://pdg.ihep.su/xsect/contents.html`. (Courtesy of the COMPAS(Protvino) and HEPDATA(Durham) Groups, March 2004. Corrections by P. Janot (CERN) and M. Schmitt (Northwestern U.))

R in Light-Flavor, Charm, and Beauty Threshold Regions

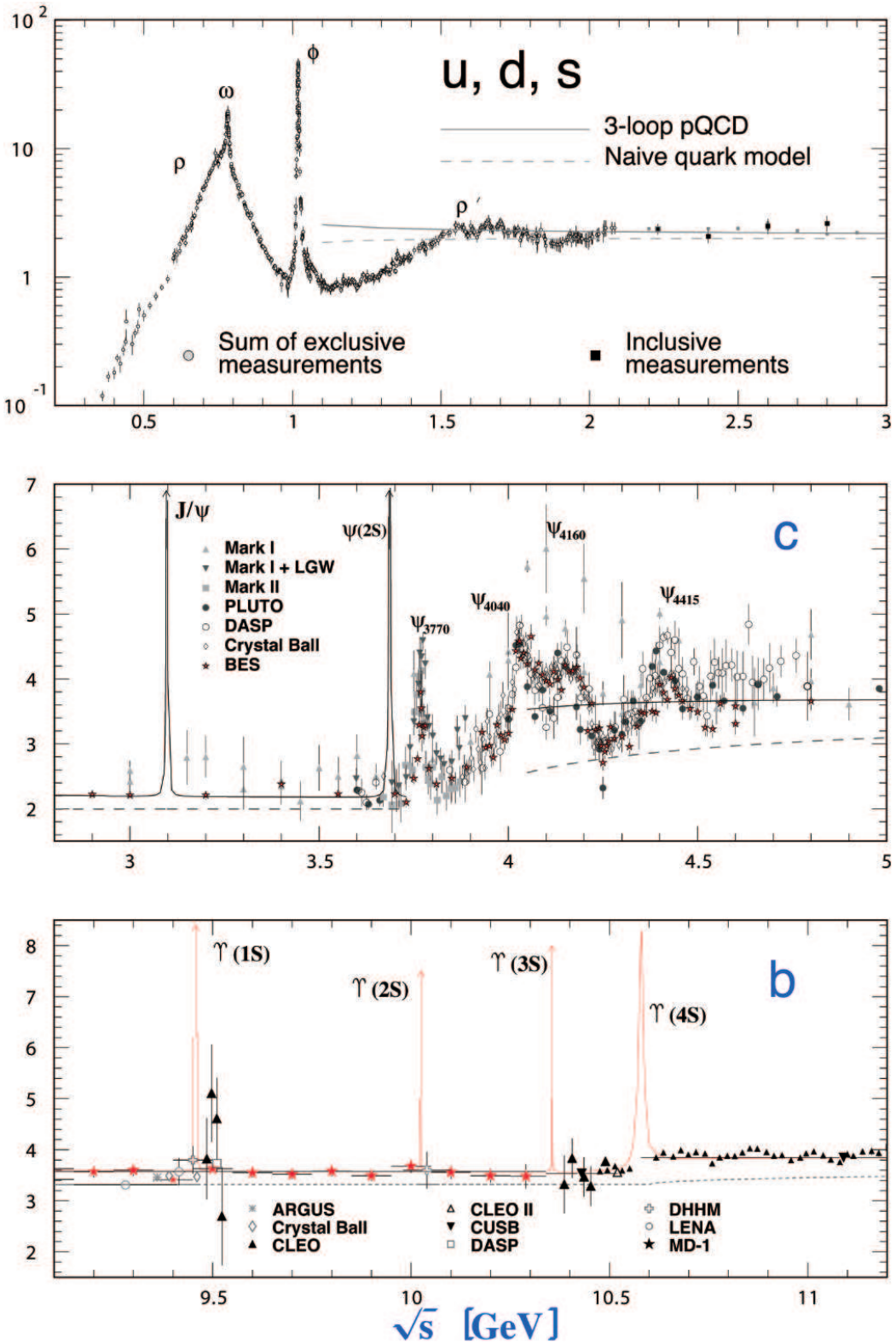

Figure 40.7: R in the light-flavor, charm, and beauty threshold regions. Data errors are total below 2 GeV and statistical above 2 GeV. The curves are the same as in Fig. 40.6. **Note:** CLEO data above $\Upsilon(4S)$ were not fully corrected for radiative effects, and we retain them on the plot only for illustrative purposes with a normalization factor of 0.8. The full list of references to the original data and the details of the R ratio extraction from them can be found in `hep-ph/0312114`. The computer-readable data are available at `http://pdg.ihep.su/xsect/contents.html` (Courtesy of the COMPAS (Protvino) and HEPDATA (Durham) Groups, March 2004.)

Annihilation Cross Section Near M_Z

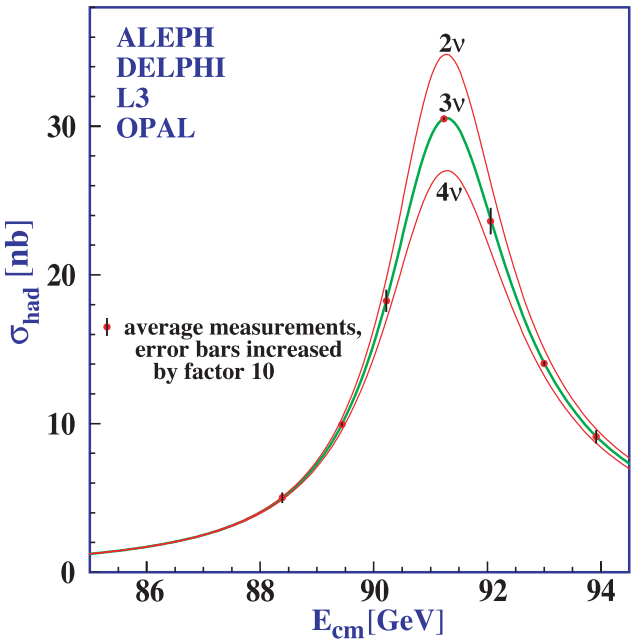

Figure 40.8: Combined data from the ALEPH, DELPHI, L3, and OPAL Collaborations for the cross section in e^+e^- annihilation into hadronic final states as a function of the center-of-mass energy near the Z pole. The curves show the predictions of the Standard Model with two, three, and four species of light neutrinos. The asymmetry of the curve is produced by initial-state radiation. Note that the error bars have been increased by a factor ten for display purposes. References:

ALEPH: R. Barate *et al.*, Eur. Phys. J. **C14**, 1 (2000).
DELPHI: P. Abreu *et al.*, Eur. Phys. J. **C16**, 371 (2000).
L3: M. Acciarri *et al.*, Eur. Phys. J. **C16**, 1 (2000).
OPAL: G. Abbiendi *et al.*, Eur. Phys. J. **C19**, 587 (2001).
Combination: The Four LEP Collaborations (ALEPH, DELPHI, L3, OPAL) and the Lineshape Sub-group of the LEP Electroweak Working Group, `hep-ph/0101027`.

(Courtesy of M. Grünewald and the LEP Electroweak Working Group, 2003)

Muon Neutrino and Anti-Neutrino Charged-Current Total Cross Section

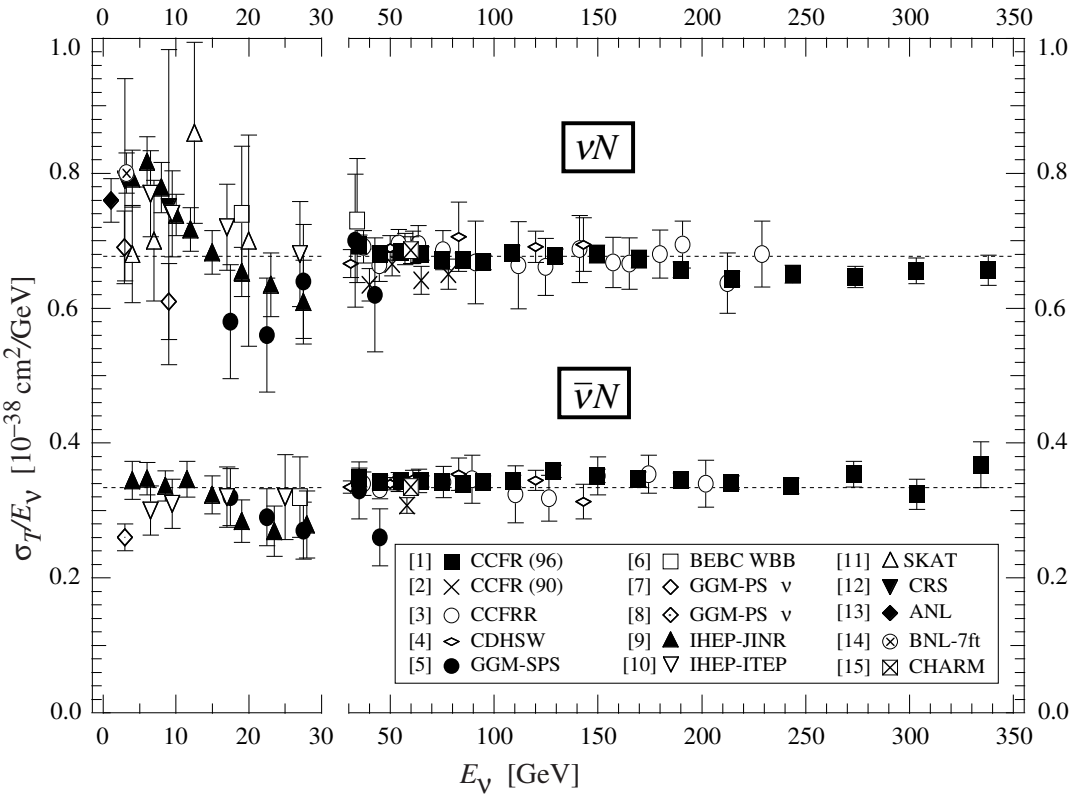

Figure 40.9: σ_T/E_ν, for the muon neutrino and anti-neutrino charged-current total cross section as a function of neutrino energy. The error bars include both statistical and systematic errors. The straight lines are the averaged values over all energies as measured by the experiments in Refs. [1–4]: $= 0.677 \pm 0.014$ $(0.334 \pm 0.008) \times 10^{-38}$ cm^2/GeV. Note the change in the energy scale at 30 GeV. (Courtesy W. Seligman and M.H. Shaevitz, Columbia University, 2001.)

[1] W. Seligman, Ph.D. Thesis, Nevis Report 292 (1996);
[2] P.S. Auchincloss *et al.*, Z. Phys. **C48**, 411 (1990);
[3] D.B. MacFarlane *et al.*, Z. Phys. **C26**, 1 (1984);
[4] P. Berge *et al.*, Z. Phys. **C35**, 443 (1987);
[5] J. Morfin *et al.*, Phys. Lett. **104B**, 235 (1981);
[6] D.C. Colley *et al.*, Z. Phys. **C2**, 187 (1979);
[7] S. Campolillo *et al.*, Phys. Lett. **84B**, 281 (1979);
[8] O. Erriquez *et al.*, Phys. Lett. **80B**, 309 (1979);
[9] V.B. Anikeev *et al.*, Z. Phys. **C70**, 39 (1996);
[10] A.S. Vovenko *et al.*, Sov. J. Nucl. Phys. **30**, 527 (1979);
[11] D.S. Baranov *et al.*, Phys. Lett. **81B**, 255 (1979);
[12] C. Baltay *et al.*, Phys. Rev. Lett. **44**, 916 (1980);
[13] S.J. Barish *et al.*, Phys. Rev. **D19**, 2521 (1979);
[14] N.J. Baker *et al.*, Phys. Rev. **D25**, 617 (1982);
[15] J.V. Allaby *et al.*, Z. Phys. **C38**, 403 (1988).

Table 40.2: Total hadronic cross section. Analytic S-matrix and Regge theory suggest a variety of parameterizations of total cross sections at high energies with different areas of applicability and fits quality.

A ranking procedure, based on measures of different aspects of the quality of the fits to the current evaluated experimental database, allows one to single out the following parameterization of highest rank[1]

$$\sigma^{ab} = Z^{ab} + B\log^2(s/s_0) + Y_1^{ab}(s_1/s)^{\eta_1} - Y_2^{ab}(s_1/s)^{\eta_2}\ , \qquad \sigma^{\overline{a}b} = Z^{ab} + B\log^2(s/s_0) + Y_1^{ab}(s_1/s)^{\eta_1} + Y_2^{ab}(s_1/s)^{\eta_2}$$

where Z^{ab}, B, Y_i^{ab} are in mb, s, s_1, and s_0 are in GeV^2. The scales s_0, s_1, the rate of universal rise of the cross sections B, and exponents η_1 and η_2 are independent of the colliding particles. The scale s_1 is fixed at 1 GeV^2. Terms $Z^{ab} + B\log^2(s/s_0)$ represent the pomerons. The exponents η_1 and η_2 represent lower-lying C-even and C-odd exchanges, respectively. Requiring $\eta_1 = \eta_2$ results in somewhat poorer fits. In addition to total cross sections σ, the measured ratios of the real-to-imaginary parts of the forward scattering amplitudes $\rho = \mathrm{Re}(T)/\mathrm{Im}(T)$ were included in the fits by using s to u crossing symmetry and differential dispersion relations. Global fits were made to the 2003-updated data for $\overline{p}(p)p$, $\Sigma^- p$, $\pi^\pm p$, $K^\pm p$, γp, and $\gamma\gamma$ collisions. Exact factorisation hypothesis was used for both Z^{ab} and $\log^2(s/s_0)$ to extend the universal rise of the total hadronic cross sections to the $\gamma p \to hadrons$ and $\gamma\gamma \to hadrons$ collisions. This resulted in reducing the number of adjusted parameters from 21 used for the 2002 edition to 19, and in the higher quality rank of the parameterization. The asymptotic parameters thus obtained were then fixed and used as inputs to a fit to a larger data sample that included cross sections on deuterons (d) and neutrons (n). All fits were produced to data above $\sqrt{s_{\min}} = 5$ GeV.

Fits to $\overline{p}(p)\,p$, $\Sigma^- p$, $\pi^\pm p$, $K^\pm p$, γp, $\gamma\gamma$			Beam/	Fits to groups				χ^2/dof
Z	Y_1	Y_2	Target	Z	Y_1	Y_2	B	by groups
35.45(48)	42.53(1.35)	33.34(1.04)	$\overline{p}(p)/p$	35.45(48)	42.53(23)	33.34(33)	0.308(10)	
			$\overline{p}(p)n$	35.80(16)	40.15(1.59)	30.00(96)	0.308(10)	1.029
35.20(1.46)	−199(102)	−264(126)	Σ^-/p	35.20(1.41)	−199(86)	−264(112)	0.308(10)	0.565
20.86(40)	19.24(1.22)	6.03(19)	$\pi^\pm/p$	20.86(3)	19.24(18)	6.03(9)	0.308(10)	0.955
17.91(36)	7.1(1.5)	13.45(40)	$K^\pm/p$	17.91(3)	7.14(25)	13.45(13)	0.308(10)	
			$K^\pm/n$	17.87(6)	5.17(50)	7.23(28)	0.308(10)	0.669
0.0317(6)			γ/p		0.0320(40)		0.308(10)	
−0.61(62)E−3			γ/γ		−0.58(61)E−3		0.308(10)	0.766
$\chi^2/dof = 0.971$,	$B = 0.308(10)$ mb,		$\overline{p}(p)/d$	64.35(38)	130(3)	85.5(1.3)	0.537(31)	1.432
$\eta_1 = 0.458(17)$,	$\eta_2 = 0.545(7)$		$\pi^\pm/d$	38.62(21)	59.62(1.53)	1.60(41)	0.461(14)	0.735
$\delta = 0.00308(2)$,	$\sqrt{s_0} = 5.38(50)$ GeV		$K^\pm/d$	33.41(20)	23.66(1.45)	28.70(37)	0.449(14)	0.814

The fitted functions are shown in the following figures, along with one-standard-deviation error bands. When the reduced χ^2 is greater than one, a scale factor has been included to evaluate the parameter values, and to draw the error bands. Where appropriate, statistical and systematic errors were combined quadratically in constructing weights for all fits. On the plots, only statistical error bars are shown. Vertical arrows indicate lower limits on the $p_{\rm lab}$ or $E_{\rm cm}$ range used in the fits.

One can find the details of the global fits (all data on proton target and $\gamma\gamma$ fitted simultaneously) and ranking procedure, as well as the exact parameterizations of the total cross sections, and corresponding ratios of the real to imaginary parts of the forward-scattering amplitudes in the recent paper of COMPETE Collab. [1]. Database used in the fits now includes the recent OPAL and L3 (LEP) $\gamma\gamma$ data, highest energy data for $\pi^- p$ and $\Sigma^- p$ from SELEX(FNAL) experiment, $\gamma\,p$ from ZEUS(DESY), cosmic ray pp data from the Fly's Eye and AKENO(Agasa), and $\gamma\,p$ data from Baksan experiments. The numerical experimental data were extracted from the PPDS accessible at `http://wwwppds.ihep.su:8001/ppds.html`. Computer-readable data files are also available at `http://pdg.lbl.gov`. (Courtesy of the COMPAS group, IHEP, Protvino, August 2003.) On-line "Predictor" to calculate σ and ρ for any energy from five high rank models is also available at `http://nuclth02.phys.ulg.ac.be/compete/predictor.html/`.

References:

1. J.R. Cudell *et al.* (COMPETE Collab.), Phys. Rev. **D65**, 074024 (2002).
2. G. Abbiendi *et al.* (OPAL Collab.), Eur. Phys. J. **C14**, 199 (2000).
3. M. Acciarri *et al.* (L3 Collab.), Phys. Lett. **B519**, 33 (2001).
4. U. Dersch *et al.* (SELEX Collab.), Nucl. Phys. **B579**, 277 (2000).
5. S. Chekanov *et al.* (ZEUS Collab.), Nucl. Phys. **B627**, 3 (2002).
6. R.M. Baltrusaitis *et al.* (Fly's Eye Collab.), Phys. Rev. Lett. **52**, 1380 (1984).
7. M. Honda *et al.* (Akeno Collab.), Phys. Rev. Lett. **70**, 525 (1993).
8. G.M. Vereshkov*et al.* (Baksan Collab.), Phys. Atom. Nucl. **66**, 565 (2003) [Yad. Fiz. **66**, 591 (2003)].

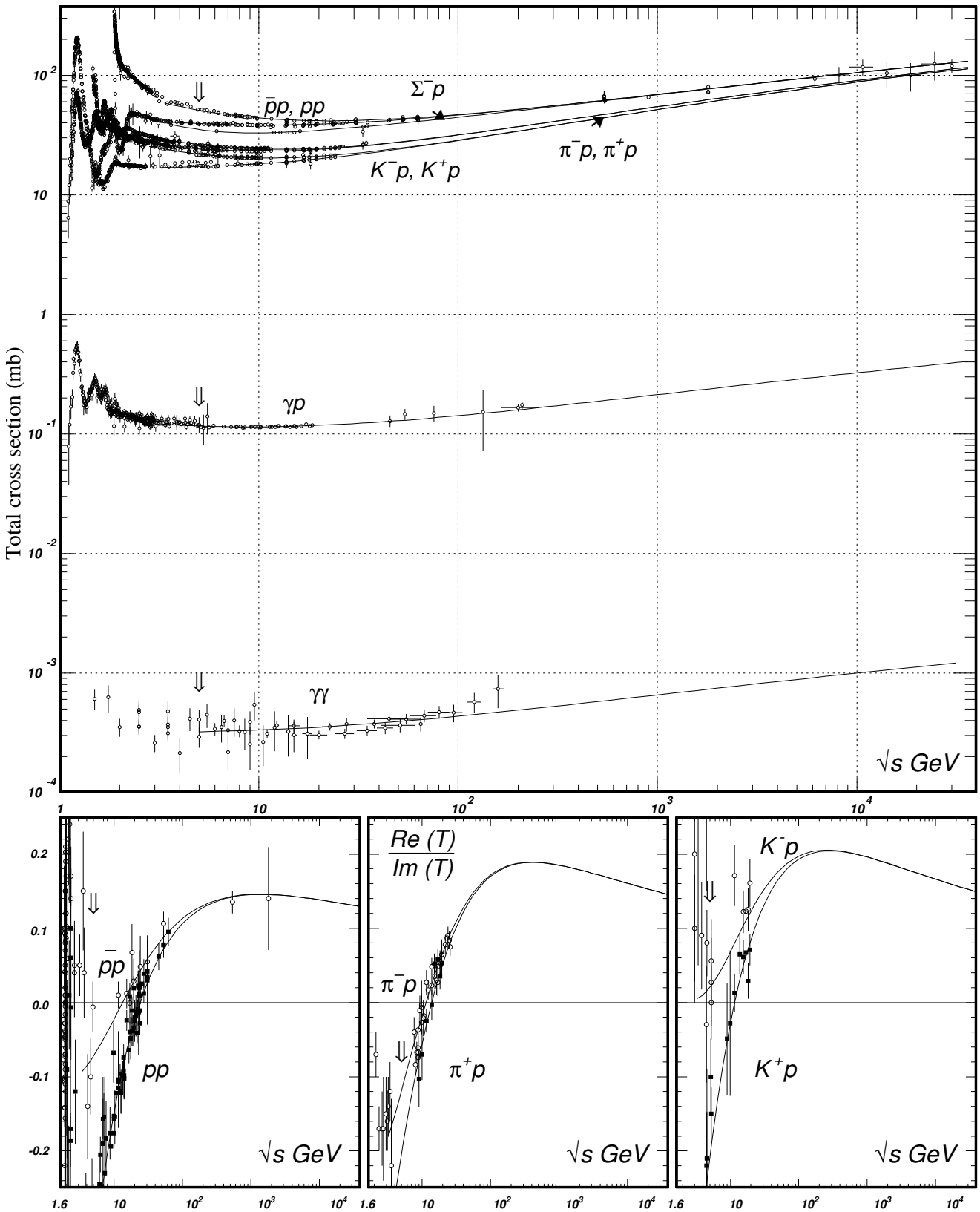

Figure 40.10: Summary of hadronic, γp, and $\gamma\gamma$ total cross sections, and ratio of the real to imaginary parts of the forward hadronic amplitudes. Corresponding computer-readable data files may be found at `http://pdg.lbl.gov/xsect/contents.html`. (Courtesy of the COMPAS group, IHEP, Protvino, August 2003.)

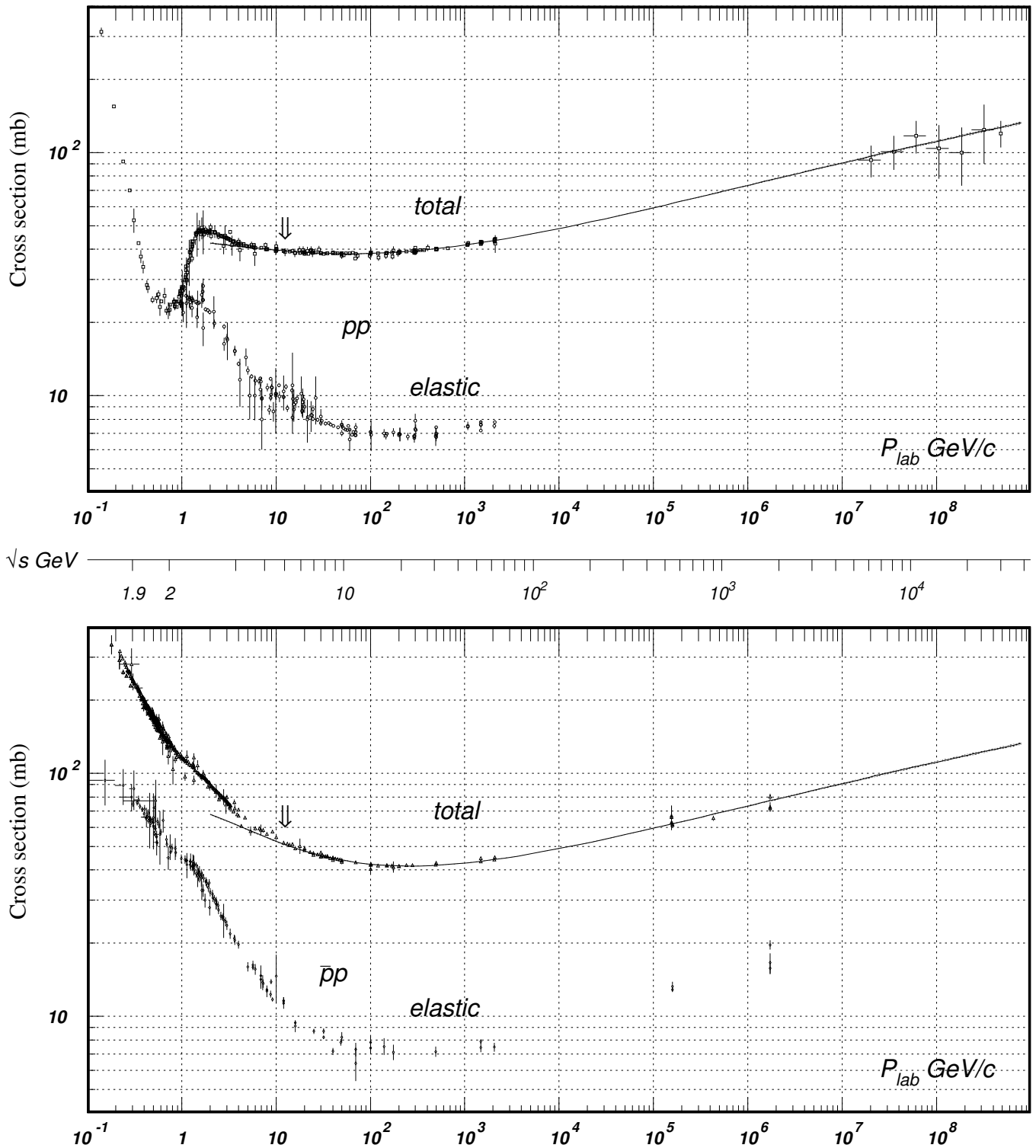

Figure 40.11: Total and elastic cross sections for pp and $\overline{p}p$ collisions as a function of laboratory beam momentum and total center-of-mass energy. Corresponding computer-readable data files may be found at `http://pdg.lbl.gov/xsect/contents.html`. (Courtesy of the COMPAS group, IHEP, Protvino, August 2003.)

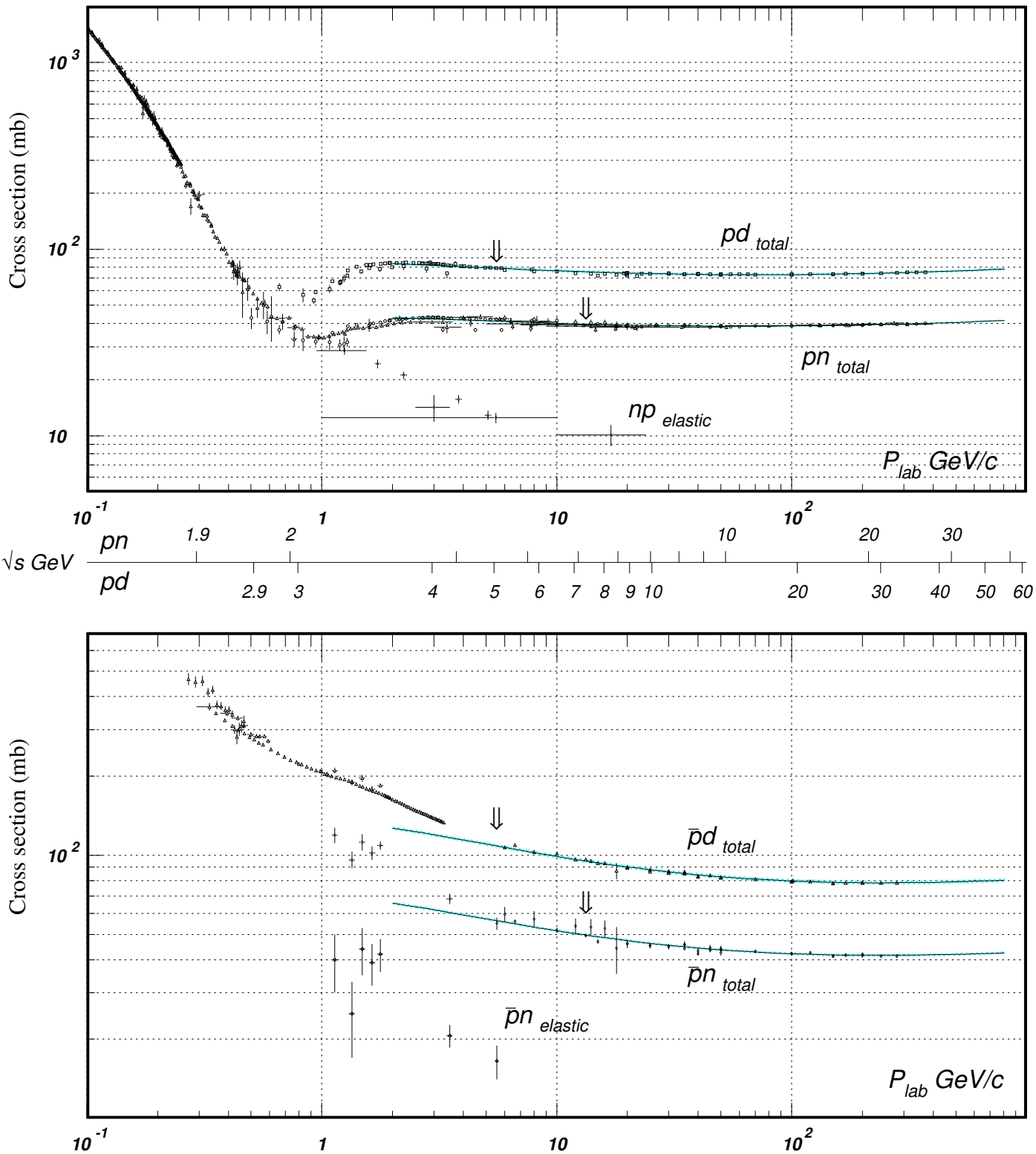

Figure 40.12: Total and elastic cross sections for pd (total only), np, $\overline{p}d$ (total only), and $\overline{p}n$ collisions as a function of laboratory beam momentum and total center-of-mass energy. Corresponding computer-readable data files may be found at `http://pdg.lbl.gov/xsect/contents.html`. (Courtesy of the COMPAS Group, IHEP, Protvino, August 2003.)

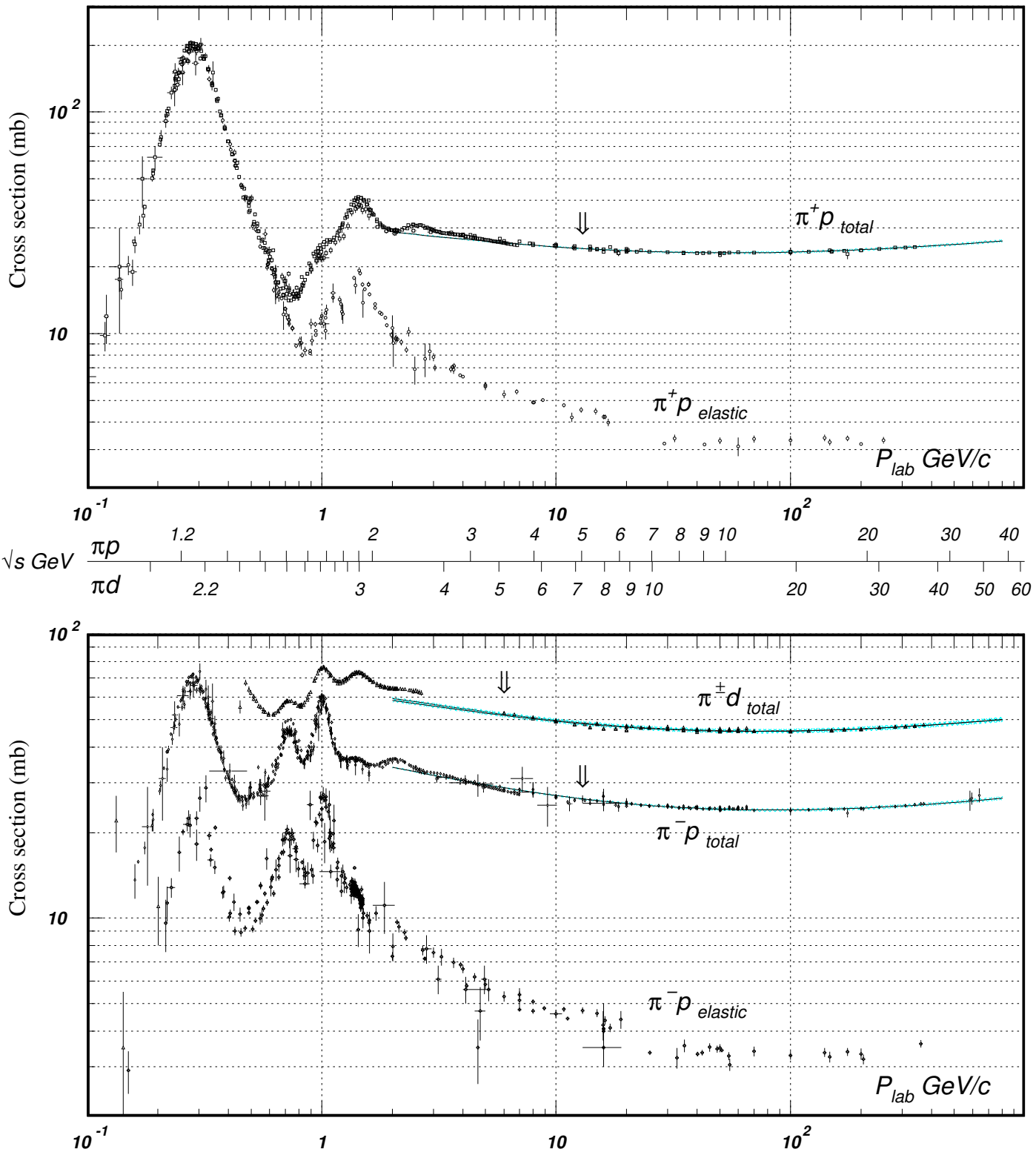

Figure 40.13: Total and elastic cross sections for $\pi^{\pm}p$ and $\pi^{\pm}d$ (total only) collisions as a function of laboratory beam momentum and total center-of-mass energy. Corresponding computer-readable data files may be found at `http://pdg.lbl.gov/xsect/contents.html`. (Courtesy of the COMPAS Group, IHEP, Protvino, August 2003.)

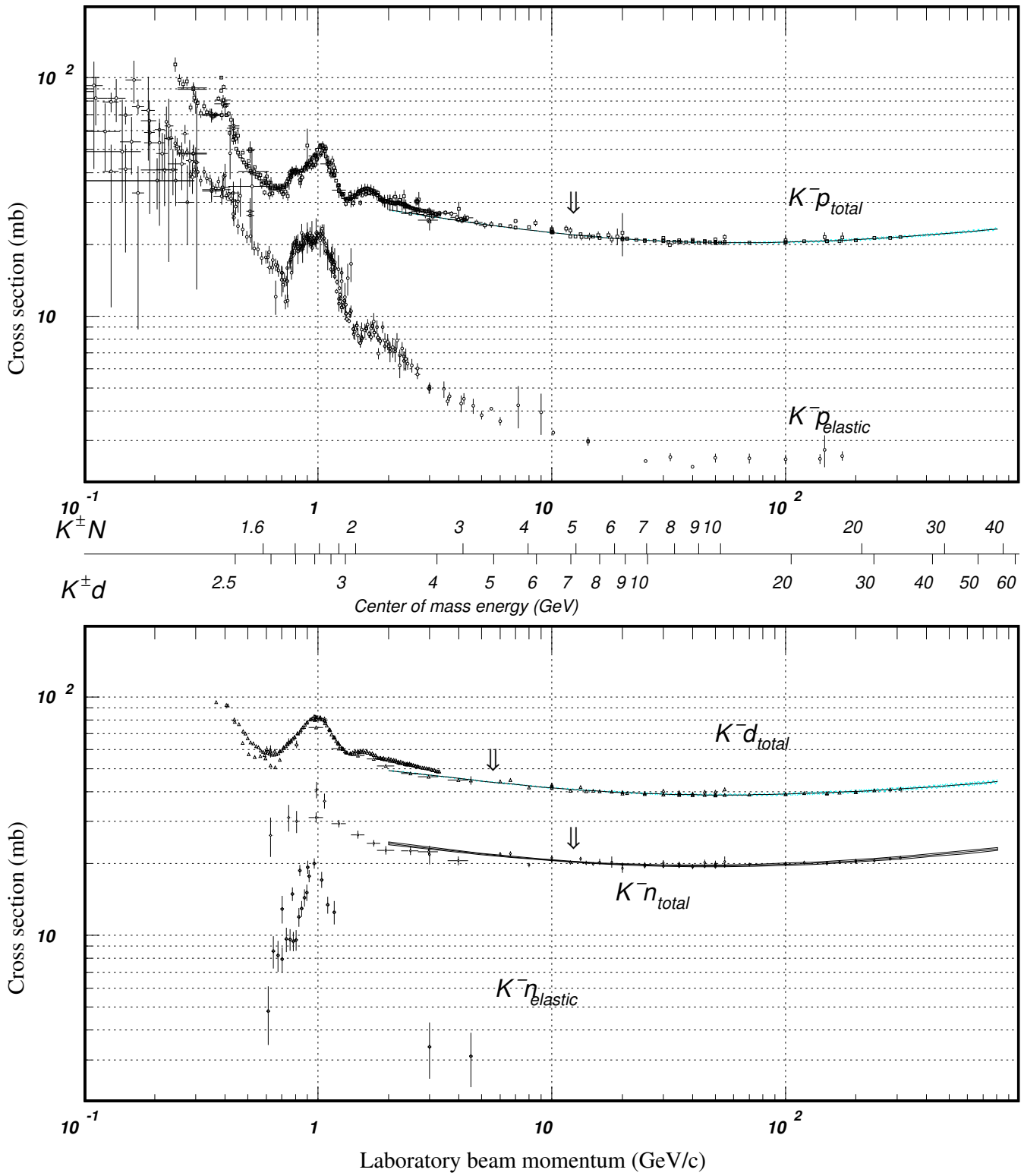

Figure 40.14: Total and elastic cross sections for $K^- p$ and $K^- d$ (total only), and $K^- n$ collisions as a function of laboratory beam momentum and total center-of-mass energy. Corresponding computer-readable data files may be found at `http://pdg.lbl.gov/xsect/contents.html`. (Courtesy of the COMPAS Group, IHEP, Protvino, August 2003.)

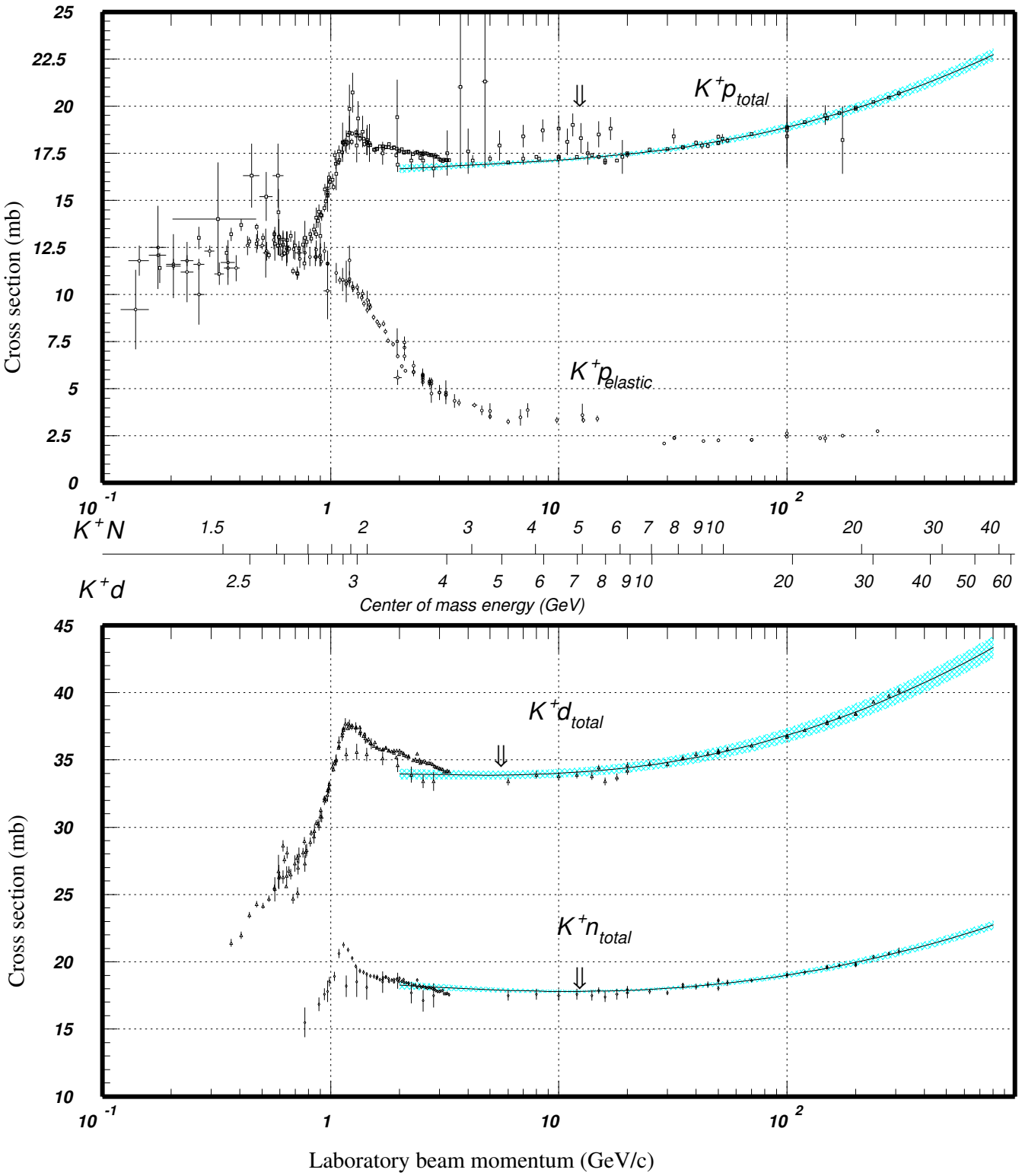

Figure 40.15: Total and elastic cross sections for K^+p and total cross sections for K^+d and K^+n collisions as a function of laboratory beam momentum and total center-of-mass energy. Corresponding computer-readable data files may be found at `http://pdg.lbl.gov/xsect/contents.html`. (Courtesy of the COMPAS Group, IHEP, Protvino, August 2003.)

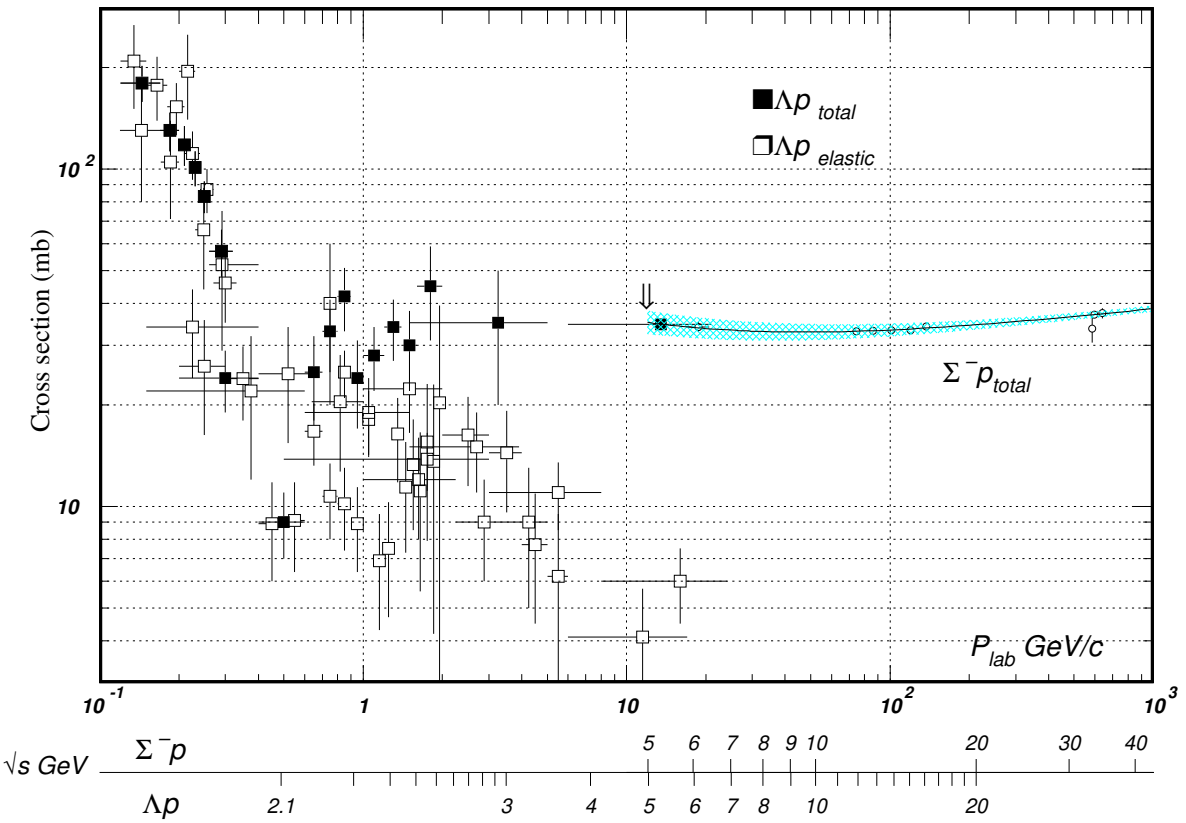

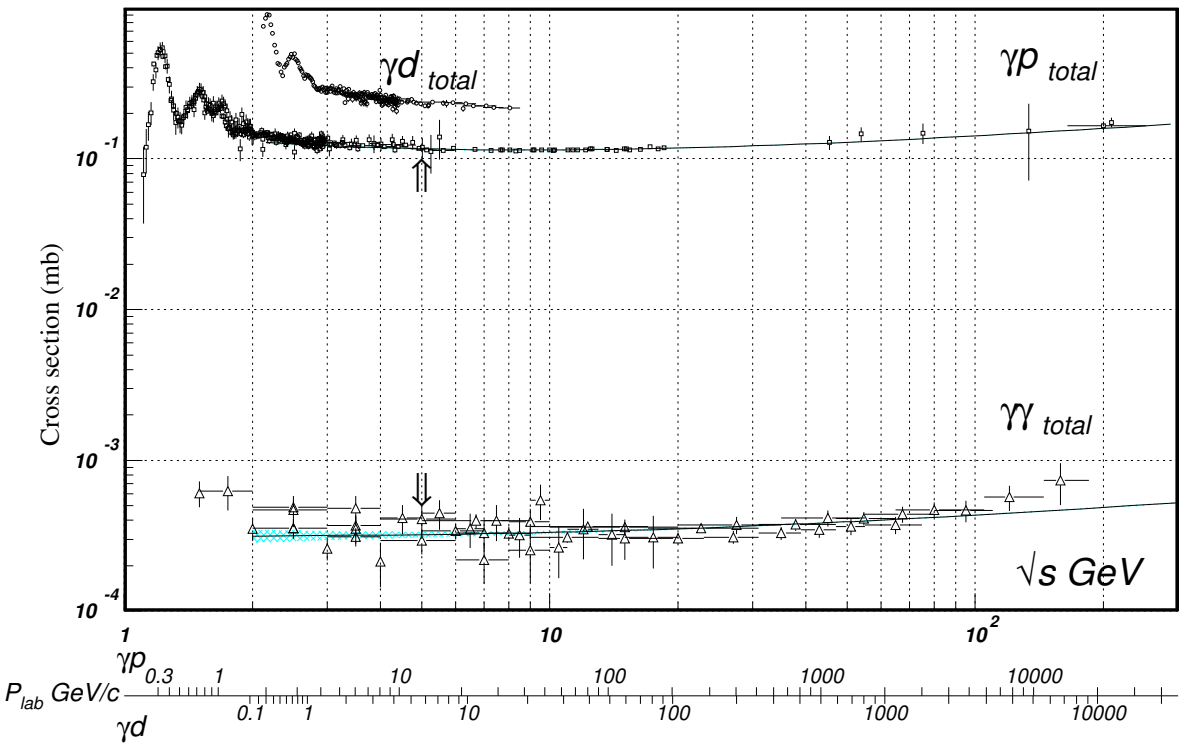

Figure 40.16: Total and elastic cross sections for Λp, total cross section for $\Sigma^- p$, and total hadronic cross sections for γd, γp, and $\gamma\gamma$ collisions as a function of laboratory beam momentum and the total center-of-mass energy. Corresponding computer-readable data files may be found at `http://pdg.lbl.gov/xsect/contents.html`. (Courtesy of the COMPAS group, IHEP, Protvino, August 2003.)